Title	Influence of growth temperature on growth of InGaAs nanowires in selective-area metal-organic vapor-phase epitaxy
Author(s)	Kohashi, Yoshinori; Sato, Takuya; Ikejiri, Keitaro et al.
Citation	Journal of Crystal Growth, 338(1), 47-51 https://doi.org/10.1016/j.jcrysgro.2011.10.041
Issue Date	2012-01-01
Doc URL	https://hdl.handle.net/2115/48549
Type	journal article
File Information	JCG338-1_47-51.pdf

Influence of Growth Temperature on Growth of InGaAs Nanowires in Selective-area Metal-organic Vapor-phase Epitaxy

Yoshinori Kohashi[a,*], Takuya Sato[a,b], Keitaroh Ikejiri[a,b], Katsuhiro Tomioka[b,c], Shinjiroh Hara[a,b], and Junichi Motohisa[a]

[a]*Graduate School of Information Science and Technology, Hokkaido University, North 14, West 9, Sapporo 060-0814, Japan*

[b]*Research Center for Integrated Quantum Electronics, Hokkaido University, North 13, West 8, Sapporo 060-8628, Japan*

[c]*JST-PREST, Japan Science and Technology Agency, Kawaguchi 332-0012, Japan*

Tel: +81-11-706-7189, Fax: +81-11-716-6004, e-mail: kohashi@impulse.ist.hokudai.ac.jp

Abstract

Indium-rich InGaAs nanowires were grown on an InP(111)B substrate by catalyst-free selective-area metal-organic vapor phase epitaxy, and its growth-temperature dependence of growth rate and composition was studied. In particular, nanowire growth rate rapidly decreases as growth temperature increases. This tendency is opposite (for a similar temperature range) to that found in a previous study on selective-area growth of gallium-rich InGaAs nanowires. This difference between indium-rich and gallium-rich nanowires suggests that the influence of growth temperature on the growth of InGaAs nanowires is dependent on the group-III supply ratio. On the basis of previous experimental observations in InAs and GaAs nanowires, temperature dependence of nanowire growth rate and its dependence on group-III supply ratio are predicted. A guideline to determine the optimum growth conditions of InGaAs nanowires is also discussed.

Keywords:

A1. Nanostructures

A3. Metalorganic vapor phase epitaxy

A3. Selective epitaxy

B2. Semiconducting III-V materials

B2. Semiconducting ternary compounds

1. Introduction

Epitaxially grown semiconductor nanowires (NWs) have generated much research interest lately because of their unique potential as building blocks of future electronic/photonic devices [1-5]. Because lattice strain allows elastic deformation without introducing misfit dislocations due to ultra-small growth regions [6], it is possible to achieve integration of III-V compound NWs on silicon platform [7]. One of the major approaches for growing NWs is a catalyst-assisted vapor-liquid-solid (VLS) method, which includes however the possibility of catalyst incorporation, leading to lower quality NWs. On the other hand, the growth of NWs by catalyst-free selective-area metal-organic vapor-phase epitaxy (SA-MOVPE) was previously reported [8-11], which is fortunately capable of forming precisely controlled NWs in terms of size, position, and growth direction and producing future nanowire-based devices [12,13] without lowering quality of the NWs. Recently, indium-rich InGaAs channel metal-insulator-semiconductor FETs (MISFETs) has been studied intensively [14,15], because of its high electron mobility and good interface properties [16], which are however very sensitive to the mole fraction of group-III atoms [17].

The key issues for growing InGaAs NWs are controlling and uniformity of their size and alloy composition. In a recent study on SA-grown InGaAs NWs [18], we obtained highly uniform NWs and found that their alloy composition was constant along their whole length, which is more favorable to VLS-grown NWs [19,20] where their alloy composition varied unacceptably. However, our previous reports on the SA-growth of InGaAs NWs are still limited to the cases where growth rate and alloy composition were investigated as a function of group-III supply ratio [21,22] at fixed temperature, and of growth temperature under gallium-rich supply condition [23]. In the present study, temperature dependence of the growth of InGaAs NWs under an indium-rich supply condition was investigated and was compared with our previous results on InAs, gallium-rich InGaAs and GaAs NWs. A guideline to find the optimum growth conditions for InGaAs NWs across the whole alloy composition range is also discussed.

2. Experimental methods

The procedure of SA-MOVPE for fabricating InGaAs NWs is explained as follows (see Fig. 1(a) and 1(b)). After a 10-nm-thick SiO_2 film is deposited on an InP (111)B substrate by RF sputtering, periodic patterns of the openings in a SiO_2 mask were defined by electron-beam (EB) lithography and wet chemical etching. The patterns consisted of circular holes with diameter, d_0, ranging from 40 to 100 nm and mask pitch, a, was 1000 nm. NWs were then formed by a horizontal MOVPE system working at 0.1 atm, supplying trimethylindium (TMIn), trimethylgallium (TMGa), and 20% arsine (AsH_3) diluted in hydrogen. The partial pressures of TMIn, [TMIn] [24] and TMGa, [TMGa] were 1.63×10^{-6} and 0.70×10^{-6} atm, giving indium-supply (group-III supply) ratio In_{supply} = [TMIn]/([TMIn]+[TMGa]) being 0.70. The partial pressure [AsH_3] of AsH_3 was 2.5×10^{-4} atm, giving V/III ratio of 107. Growth temperature, T_G, and growth time, t, were varied from 590 to 650°C and 10 to 90 min, respectively.

Height, *h*, and diameter, *d*, of the NWs were measured by scanning-electron microscopy (SEM). Alloy composition of NWs was estimated by micro-photoluminescence (μ-PL) measurement at 4K. Excitation light from $TiAl_2O_3$ laser operating at 773 nm was focused on NW arrays by ×20 microscope objectives with a numerical aperture of 0.40, which was also used to collect the PL from the NWs.

3. Experimental results

3.1. Growth of indium-rich InGaAs nanowires

Figure 1(c) shows a typical SEM image of InGaAs NWs grown by SA-MOVPE. Growth temperature, T_G, and growth time, *t*, were 635°C and 30 min, respectively, with opening diameter, d_0, of 100 nm. We can see that highly uniform and non-tapered NWs. In addition, these NWs have six sidewall {-110} facets normal to the (111)B plane in a similar manner to the cases of InAs, gallium-rich InGaAs, and GaAs NWs [10,11,23]. Similar NWs were observed for T_G from 590°C to 650°C.

It is noted here that the present study differs from our previous report on gallium-rich InGaAs NWs (In_{supply} = 0.08) in one respect [23]. Previously, particle-like depositions were found on the mask-opening regions for the samples grown at T_G from 600 to 650°C. The density of particle-like depositions decreased as T_G increased, and the depositions disappeared at T_G of 700°C. These particle-like depositions were not confirmed in the case of the present study (In_{supply} = 0.70), in aforementioned temperature range.

3.2. Temperature dependence of nanowire size

Figure 2 shows temperature dependence of NW height, h, and diameter, d, at each d_0 for t = 30 min. It is clear that h significantly decreases as T_G increases, particularly above 620°C. This result can be explained by an increase of desorption of constituent atoms from NWs or re-evaporation of precursors from masked area with increasing T_G [10,11].

It should be noted that this trend is in contrast to the results of gallium-rich NWs (In_{supply} = 0.08) [23], where higher T_G resulted in increased h from T_G = 600 to 700°C. Namely, temperature dependence of h is quite different in the cases of indium-rich and gallium-rich NWs in the same T_G range. In addition, in Ref. [23], NW diameter, d, was larger than d_0, and it appeared to be independent of T_G. This is also in contrast to the result of the present study, where d clearly dependent on T_G, particularly above 620°C and lateral growth is negligible at 650°C.

3.3. Time evolution of nanowire size

As shown in Fig. 2(b), significant lateral growth was observed in the samples grown below 635°C. To identify the origin of this lateral growth, the time evolution of NW size was studied (see Fig. 3). The figure shows superlinear evolution of h for shorter t, and almost linear evolution for longer t. In addition, the lateral growth became significant after a certain amount of growth. This result is similar to our previous results presented in Ref. [21], where time evolution of the NW size was explained by a model based on a diffusion of growth species. In this model, it was argued that the lateral growth took place when h becomes larger than the critical length, which is determined by the diffusion length on the sidewalls of the NWs. We consider that the present results of time evolution of NW size can also be explained by the same model. The origin of the lateral growth is therefore mainly due to excessive growth time, and it can be ignored when an appropriate growth time is used.

Beside, as shown in Fig. 2, h and d are not dependent on d_0. This independence is also due to the excessive growth time, since long-term growth over the critical NW length will enlarge d and eventually result in a similar NW size independently of d_0. Note, however, that it implies that the lateral growth was more enhanced in the initial stage of growth for smaller d_0. To confirm this implication, more experiments on dependence on d_0 and growth time are necessary and left for future study.

3.4. Temperature dependence of indium composition

Figure 4(a) shows alloy composition of NWs, plotted as a function of T_G with d_0 = 100 nm. The alloy compositions and their error bars were estimated from PL-peak-energy position and full width at half maximum (FWHM) [25]. It was found that NW composition is clearly dependent on T_G, where indium composition increases from 64% to 90% as T_G decreases. It is noted that this composition dependence on T_G is similar to that in the case of gallium-rich

NWs (In_{supply} = 0.08) [23]. In Ref. [23], composition dependence on T_G was explained by arsenic trimers on the (111)B plane. As for GaAs, its (111)B surface was partially covered by arsenic trimers [26], and this stable coverage increases as temperature decreases [27]. The increase of this coverage hinders gallium atoms from absorbing onto the (111)B surface [8,9], while indium absorption is less influenced by arsenic trimers [11]. As a result, it became difficult for gallium atoms, compared to indium atoms to incorporate into the NW top facet. Simultaneously, h decrease as T_G decreases in gallium-rich InGaAs NWs as we have mentioned in section 3.2. In addition, d_0 dependence of composition was absent for T_G = 590 and 650°C (not shown here) in the present study, as reported in Ref. [23].

From h and composition dependence on T_G, the contributions of InAs and GaAs included to InGaAs NW height for d_0 = 100 nm were estimated (see Fig 4(b)). The figure shows that InAs contribution is strongly dependent on T_G. On the other hand, the GaAs contribution is slightly dependent on T_G. This result suggests that the composition dependence on T_G is attributable to larger desorption of indium atoms compared with that of gallium atoms [11]. It is thus, we considered that, contrary to the case of gallium-rich NW growth, composition dependence does not relate to arsenic trimers in the case of indium-rich NW growth.

4. Discussions

4.1. Composition-dependent behavior of temperature dependence

In the previous section, it was shown that indium-rich InGaAs NWs exhibited different growth behavior to that of gallium-rich NWs under varied growth temperature, T_G. When T_G increases, the axial (vertical) growth rate corresponded with NW height, h, reduced drastically in indium-rich NWs. This reduction is attributable to the InAs contribution, which indicates the less incorporation of indium. Meanwhile, the axial growth rate increases in gallium-rich NWs due to enhancement of GaAs growth at higher T_G. It is noted that these two behaviors are observed in the same T_G range, indicating that temperature dependence of the growth rate is significantly influenced by the group-III supply ratio, In_{supply} .

To further emphasize composition-dependent behavior, the axial growth rate for the InAs and GaAs NWs are compared with those for the indium-rich and gallium-rich InGaAs NWs in Fig. 5. The data includes results from previous reports [10,11,23] and unpublished data for GaAs NWs. The axial growth rate is normalized with group-III supply. The lines are eye guides. Because the actual growth rate depends on various factors (for instance, V/III ratio, pitch a [8], and group-III supply ratio [21]), the vertical scale is shown as an arbitrary scale. As mentioned in the previous section, quite different trends in temperature dependence for the indium-rich and gallium-rich InGaAs NWs are shown. On the other hand, interestingly, common and systematic trends are confirmed in the cases of the InAs and GaAs NWs. That is, the axial growth rate increases as T_G increases until certain temperature, T_{GC}, above which axial growth rate decreases as T_G increases. T_{GC} for InAs and GaAs are about 540 and 700°C, respectively.

In the higher T_G range (i.e., $T_G > T_{GC}$), highly uniform NWs were observed [10,11]. Furthermore, d was similar to d_0, indicating that the lateral growth was suppressed effectively. Note that the optimum growth temperature for InAs and GaAs NWs were thus concluded to be in about 540 and 750°C, respectively. In addition, in this T_G range, axial growth rate decreases as T_G increases, where it is probably due to the fact that desorption of constituent atoms from the NW top facet increases as T_G increases [11]. In regard to GaAs NWs [10], this behavior was explained by less incorporation of gallium due to reduced frequency of introduction of stacking faults. It is noted that less incorporation should be accompanied by desorption of constituent atoms in SA-MOVPE.

In the lower temperature range (i.e., $T_G < T_{GC}$), on the other hand, unfavorable growth was observed. In the case of InAs NWs [11], the uniformity of NWs was deteriorated, and considerable lateral overgrowth took place. This behavior is thought to be due to the preferential incorporation of growth species into the side walls of NWs, resulting in suppression of axial growth. On the other hand, in the growth of GaAs NWs at 650°C, their height was much shorter than those grown at 700°C, and hillocks or particle-like depositions were observed in some part of the mask opening. Reduction of axial growth rate can be explained by arsenic trimers, which prevents incorporation of gallium.

Because it is an alloy, the temperature dependence of the axial growth rate of InGaAs

NWs has a peak as the cases of InAs and GaAs NWs, and it is plausible that growth behavior becomes closer to the case of InAs (GaAs) when the NWs are indium (gallium)-rich. Consequently, T_{GC} and growth behavior exhibited in InAs and GaAs NW growth exhibits a shift in accordance with In_{supply}. It explains an apparent opposite growth behavior in the cases of indium-rich and gallium-rich NWs, where it was observed in the same T_G range. Furthermore, it also explains the results presented in Ref. [21], which was carried out at fixed T_G and found that axial growth rate decreases as In_{supply} increases.

As discussed in section 3.1, no particle-like depositions were observed in the present study, whereas they were observed in the case of gallium-rich NWs, even though both were grown in the same T_G range. As mentioned above, similar deposition was observed in GaAs grown at 650°C, but it was eliminated above 700°C. The formation or absence of particle-like depositions can be distinguished by the growth temperature, namely, whether it is below or above T_{GC}.

4.2. Optimum growth temperature for InGaAs NWs

As summarized in section 4.1, axial growth rate of a NW depends both on T_G and group-III supply ratio, In_{supply}. This dependence is thought to be correlated with to the optimum growth temperature for InGaAs NW grown under any group-III supply condition. More specifically, it is expected that the optimum growth temperature for obtaining highly uniform and thinner NWs would be in a slightly higher temperature range than T_{GC}, where the axial growth rate is maximum, for the following reasons. For growth of NWs, it is important to achieve reasonably high growth rate. In addition, lateral growth should be suppressed to obtain sufficiently thin NWs. Furthermore, we have to avoid anomalous growth such as particle-like depositions or hillocks. The first requirement can be satisfied by employing a T_G close to T_{GC}, and the second and third ones require higher T_G. The result shown in Fig. 3 strongly suggests that it is possible to form NWs with sufficient length without lateral growth (i.e., d = 100 nm and h = 3 μm), so long as growth time (thus, h) is not long. In fact, the results of Fig. 3 are obtained for T_G = 635°C, which is slightly above T_{GC}. Moreover, it was concluded empirically that optimum growth temperature for InAs and GaAs is the similar or higher than T_{GC} [10,11]. This fact also validates the present discussion on the relationship between T_{GC} and optimum growth temperature in NWs.

As shown in section 3.4, indium composition decreases as T_G increases. In addition, composition also depends on mask pitch, a [22]. Further experiments are thus necessary for obtaining NWs with the desired alloy composition of InGaAs. Other growth conditions, such as V/III ratio, might also give some effect on the growth. Nevertheless, we expect that the qualitative trends summarized in section 4.1 does not alter and offer a good guiding principle to find the optimum growth conditions for InGaAs NWs across the whole alloy composition range.

5. Summary

Growth of InGaAs NWs under an indium-rich supply condition by SA-MOVPE was investigated, and highly uniform and non-tapered NWs were thereby formed. By comparison with previous reports on InAs, gallium-rich InGaAs, and GaAs NWs, it was found that the axial growth rate of InGaAs NWs becomes maximum at a certain temperature, T_{GC}, which decreases as group-III supply ratio, In_{supply}, increases. Furthermore, it is expected that the optimum growth temperature range for InGaAs NWs lies slightly above T_{GC}, where reasonable axial growth rate is guaranteed and lateral growth is negligible. To confirm this expectation, more systematic study on, for instance, dependences on V/III ratio, mask opening size, and opening pitch are required. In addition, temperature also affects the alloy composition of NWs; thus, more accurate assessment of growth condition is required to obtain InGaAs with desired composition.

Acknowledgments

The authors thank Professor T. Fukui, Professor K. Hiruma, and M. Yoshimura for their helpful discussions, and K. Komagata, K. Morita, and S. Fujisawa for supporting the experiments. This work was financially supported by a Grant-in-Aid for Scientific Research from the Ministry of Education, Culture, Sports, Science and Technology and in part by the Global COE Program "Center for Next-Generation Information Technology based on Knowledge Discovery and Knowledge Federation", MEXT, Japan.

References

[1] J. Xiang, Wei Lu, Y. Hu, Y. Wu, H. Yan, C.M. Lieber, Naure Lett., **441** (2006) 489.

[2] Q.-T. Do, K. Blekker, I. Regolin, W. Prost, F.J. Tegude, IEEE Electron Dev. Lett., **28** (2007) 682.

[3] C. Thelander, C. Rehnstedt, L.E. Fröberg, E. Lind, T. Mårtensson, P. Caroff, T. Löwgren, B.J. Ohlsson, L. Samuelson, L.-E. Wernersson, IEEE Trans. Elect. Devices, **55** (2008) 3030.

[4] C.P.T. Svensson, T. Mårtensson, J. Trägårdh, C. Larsson, M. Rask, D. Hessman, L. Samuelson, J. Ohlsson, Nanotechnol., **19** (2008) 305201.

[5] B. Tian, X. Zheng, T.J. Kempa, Y. Fang, N. Yu, G. Yu, J. Huang, C.M. Lieber, Nature Lett., **449** (2007) 885.

[6] F. Glas, Phys. Review B, **74** (2006) 121302.

[7] T. Mårtensson, C.P.T. Svensson, B.A. Wacaser, M.W. Larsson, W. Seifert, K. Deppert, A. Gustafsson, L.R. Wallenberg, L. Samuelson, Nano Lett., **4** (2004) 1987.

[8] J. Noborisaka, J. Motohisa, T. Fukui, Appl. Phys. Lett., **86** (2005) 213102.

[9] K. Ikejiri, J. Noborisaka, S. Hara, J. Motohisa, T. Fukui, J. Cryst. Growth, **298** (2007) 616.

[10] K. Ikejiri, T. Sato, H. Yoshida, K. Hiruma, J. Motohisa, S. Hara, T. Fukui, Nanotechnol., **19** (2008) 265604.

[11] K. Tomioka, P. Mohan, J. Noborisaka, S. Hara, J. Motohisa, T. Fukui, J. Cryst. Growth, **298** (2007) 644.

[12] H. Goto, K. Nosaki, K. Tomioka, S. Hara, K. Hiruma, J. Motohisa, T. Fukui, Appl. Phys. Exp., **2** (2009) 035004.

[13] T. Tanaka, K. Tomioka, S. Hara, J. Motohisa, E. Sano, T. Fukui, Appl. Phys. Exp., **3** (2010) 025003.

[14] Y. Xuan, P.D. Ye, T. Shen, Appl. Phys. Lett., **91** (2007) 232107.

[15] Y. Xuan, Y.Q. Wu, P.D. Ye, IEEE Elect. Dev. Lett., **29** (2008) 294.

[16] H. Hasegawa, M. Akazawa, Appl. Surf. Science, **254** (2008) 8005.

[17] H.H. Wieder, H. Sari, J. Vac. Sci. Technol. B, **20** (2002) 1759.

[18] M. Yoshimura, K. Tomioka, K. Hiruma, S. Hara, J. Motohisa, T. Fukui, J. Cryst. Growth, **315** (2011) 148.

[19] Y. Kim, H.J. Joyce, Q. Gao, H.H. Tan, C. Jagadish, M. Paladugu, J. Zou, A.A. Suvorova, Nano Lett., **6** (2006) 599.

[20] F. Jabeen, S. Rubini, F. Martelli, Microelect. J., **40** (2009) 442.

[21] T. Sato, J. Motohisa, J. Noborisaka, S. Hara, T. Fukui, J. Cryst. Growth, **310** (2008) 2359.

[22] T. Sato, Y. Kobayashi, J. Motohisa, S. Hara, T. Fukui, J. Cryst. Growth, **310** (2008) 5111.

[23] M. Yoshimura, K. Tomioka, K. Hiruma, S. Hara, J. Motohisa, T. Fukui, Jpn. J. Appl. Phys., **49** (2010) 04DH08.

[24] D.V. Shenai-Khatkhate *et al.* reported an update for vapor pressure equation TMIn (D.V. Shenai-Khatkhate, R.L. DiCarlo Jr., R.A. Ware, *J. Cryst. Growth*, **310** (2008) 2395, i.e., $\log P(\text{Torr}) = 10.98\text{-}3204/T(\text{K})$). Following their equation, [TMIn] is 0.99×10^{-6} atm, giving

In_{supply} = 0. 59, and V/III = 148. In this paper, we used [TMIn] obtained by an older equation (i.e., $\log P$(Torr) = 10.52-3014/T(K)) for comparison with our previous reports.

[25] S. Paul, J.B. Roy, P.K. Basu, J. Appl. Phys., **69** (1991) 827.

[26] D.K. Biegelsen, R.D. Bringans, J.E. Northrup, L.-E. Swartz, Phys. Rev. Lett., **65** (1990) 452.

[27] T. Nishida, K. Uwai, Y. Kobayashi, N. Kobayashi, Jpn. J. Appl. Phys., **34** (1995) 6326.

Figure captions

Fig. 1. SA-MOVPE method for forming InGaAs NW array : (a) definition of opening patterns using EB lithography and wet chemical etching, (b) MOVPE growth of InGaAs NWs, and (c) SEM image of InGaAs NWs grown at 635°C. The insets show a top view of the NWs. The white scale bar represents 100 nm. [Growth conditions: t = 30 min; d_0 = 100 nm]

Fig. 2. Growth-temperature dependence of nanowire (a) height, h, and (b) diameter, d. The dashed line of inset (b) shows d_0. The error bars show maximum and minimum. [Growth conditions: t = 30 min; d_0 = 40–100 nm]

Fig. 3. Time evolution of nanowire height, h, and nanowire diameter, d. Closed squares and closed triangles represent h and d, respectively. The dashed line shows d_0. [Growth conditions: T_G = 635°C; d_0 = 100 nm]

Fig. 4. (a) Growth-temperature dependence of gallium (Ga) or indium (In) composition of InGaAs NWs. The error bar shows FWHM. (b) InAs and GaAs contributions in nanowire height, and total height of InGaAs NW. [Growth conditions: t = 30 min; d_0 = 100nm]

Fig. 5. Comparison of temperature dependence of normalized axial growth rate. From the left side of the figure, closed triangles, closed diamonds, closed circles, and closed squares, represent InAs NWs [11] (d_0 = 150 nm; a = 400 nm; t = 20 min), In-rich InGaAs NWs (present study, d_0 = 100 nm; a =1000 nm; t = 30 min), Ga-rich InGaAs NWs [23] (d_0 = 200 nm; a = 1000 nm; t = 30 min), and GaAs NWs [10] (d = 200 nm; a = 2000 nm; t = 10 min), i.e., In_{supply} = 1, 0.70, 0.08, and 0, respectively.

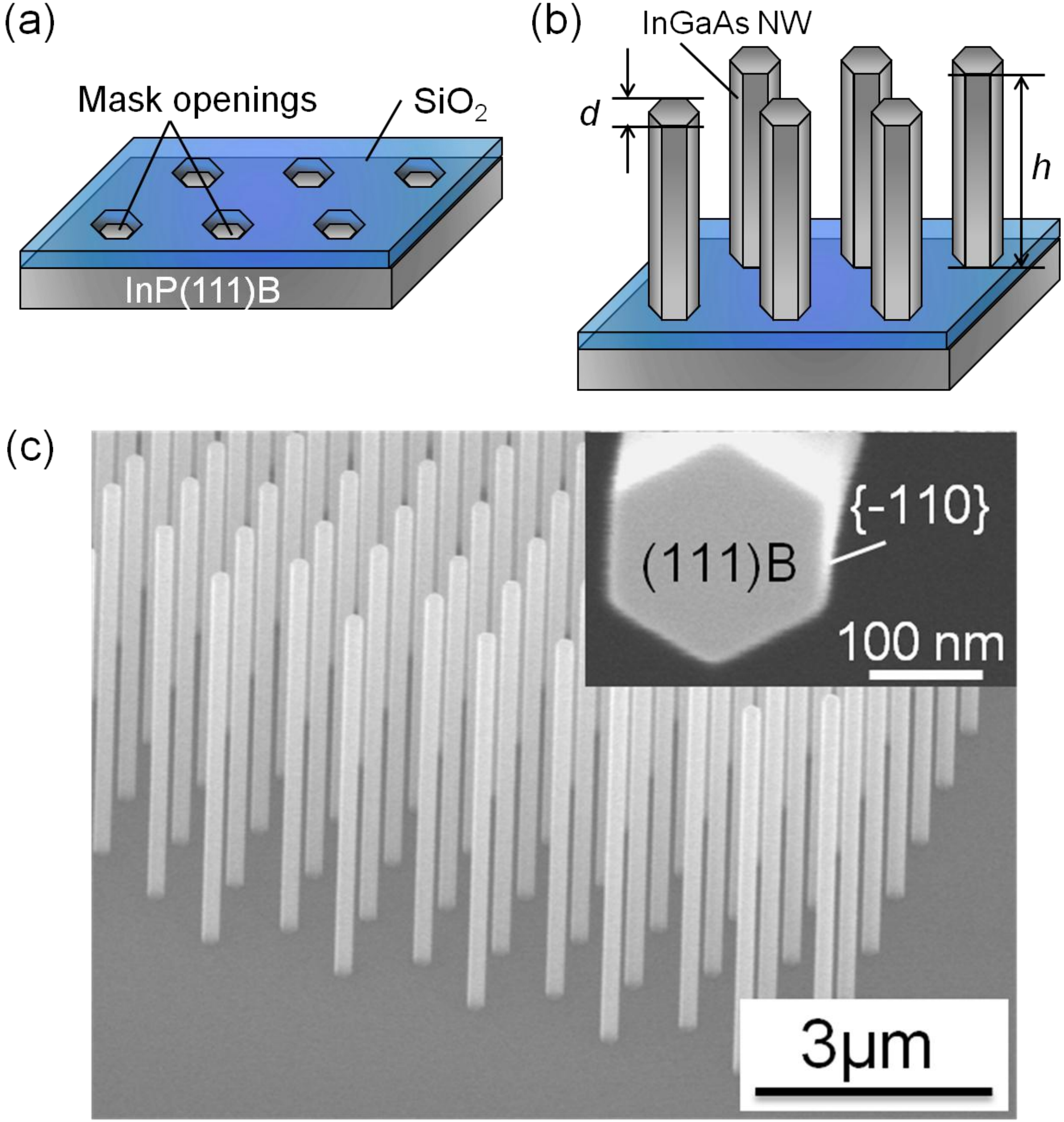
(a)
Mask openings
SiO$_2$
InP(111)B
(b)
InGaAs NW
d
h
(c)
{-110}
(111)B
100 nm
3μm

Figure 2

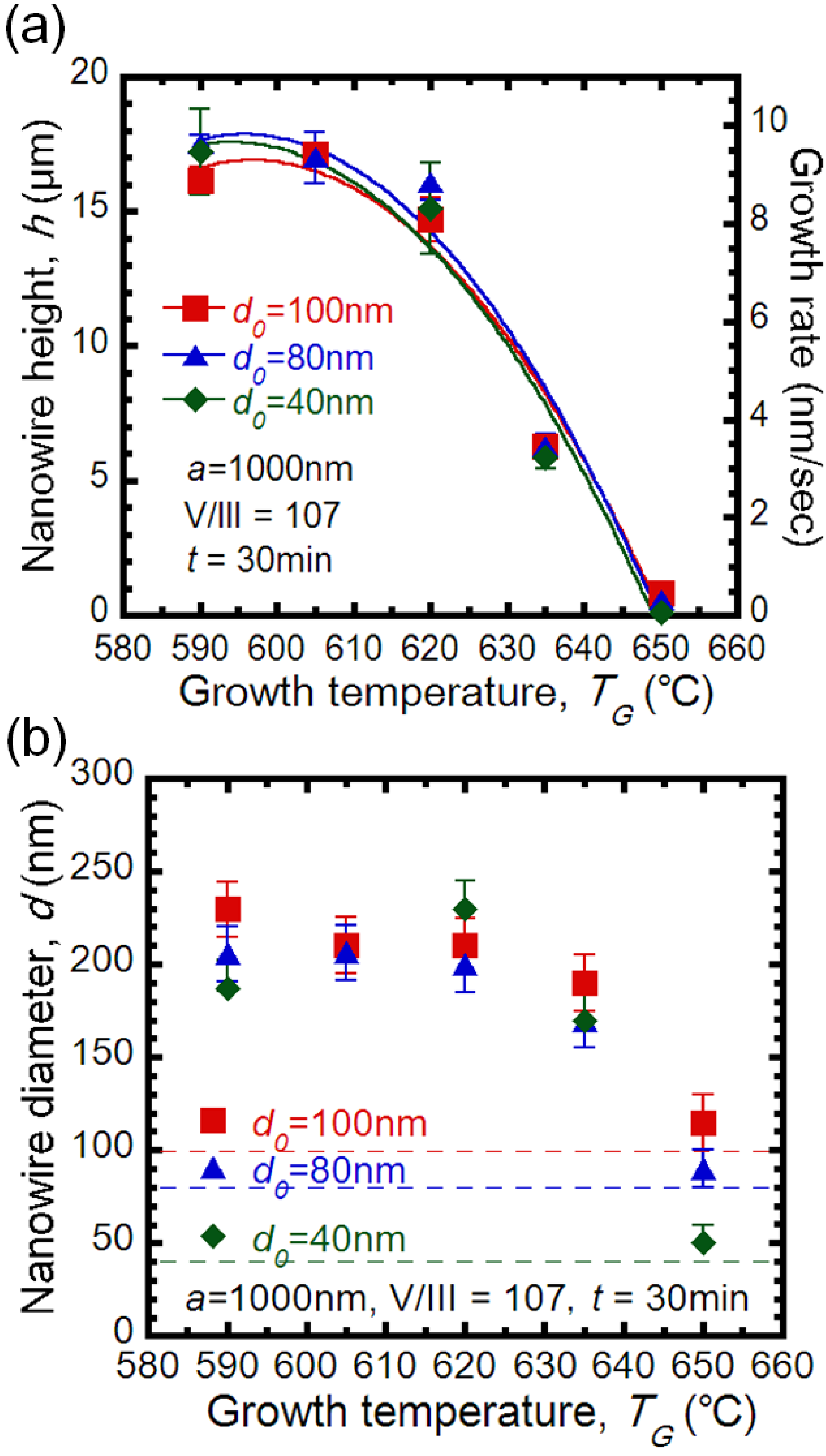
(a)
Nanowire height, h (µm)
Growth rate (nm/sec)
Growth temperature, T_G (°C)
0
5
10
15
20
0
2
4
6
8
10
580
590
600
610
620
630
640
650
660
d_0=100nm
d_0=80nm
d_0=40nm
a=1000nm
V/III = 107
t = 30min
(b)
Nanowire diameter, d (nm)
Growth temperature, T_G (°C)
0
50
100
150
200
250
300
580
590
600
610
620
630
640
650
660
d_0=100nm
d_0=80nm
d_0=40nm
a=1000nm, V/III = 107, t = 30min

Figure 3

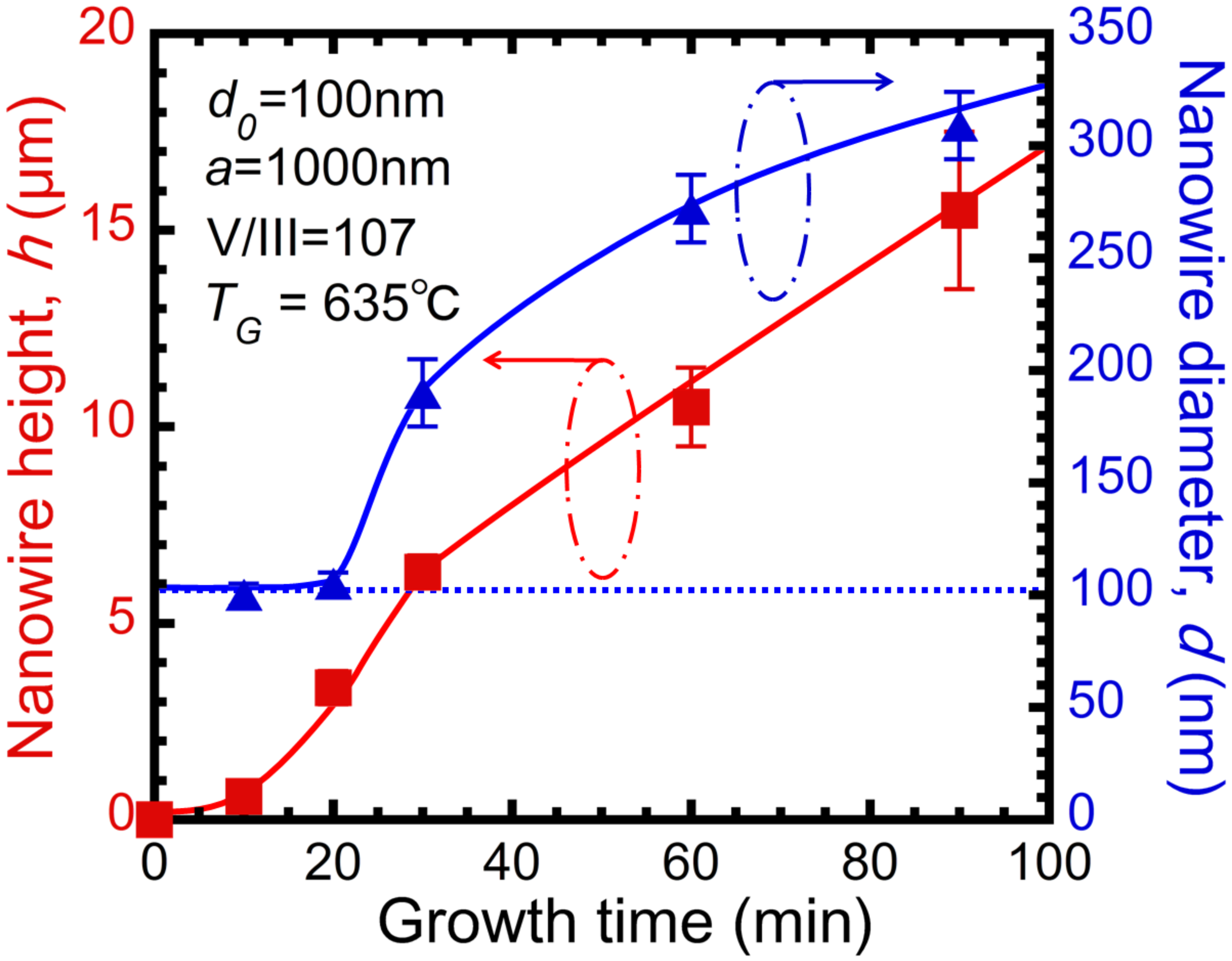
d_0=100nm
a=1000nm
V/III=107
T_G = 635°C
Nanowire height, h (μm)
0
5
10
15
20
Nanowire diameter, d (nm)
0
50
100
150
200
250
300
350
0
20
40
60
80
100
Growth time (min)

Figure 4

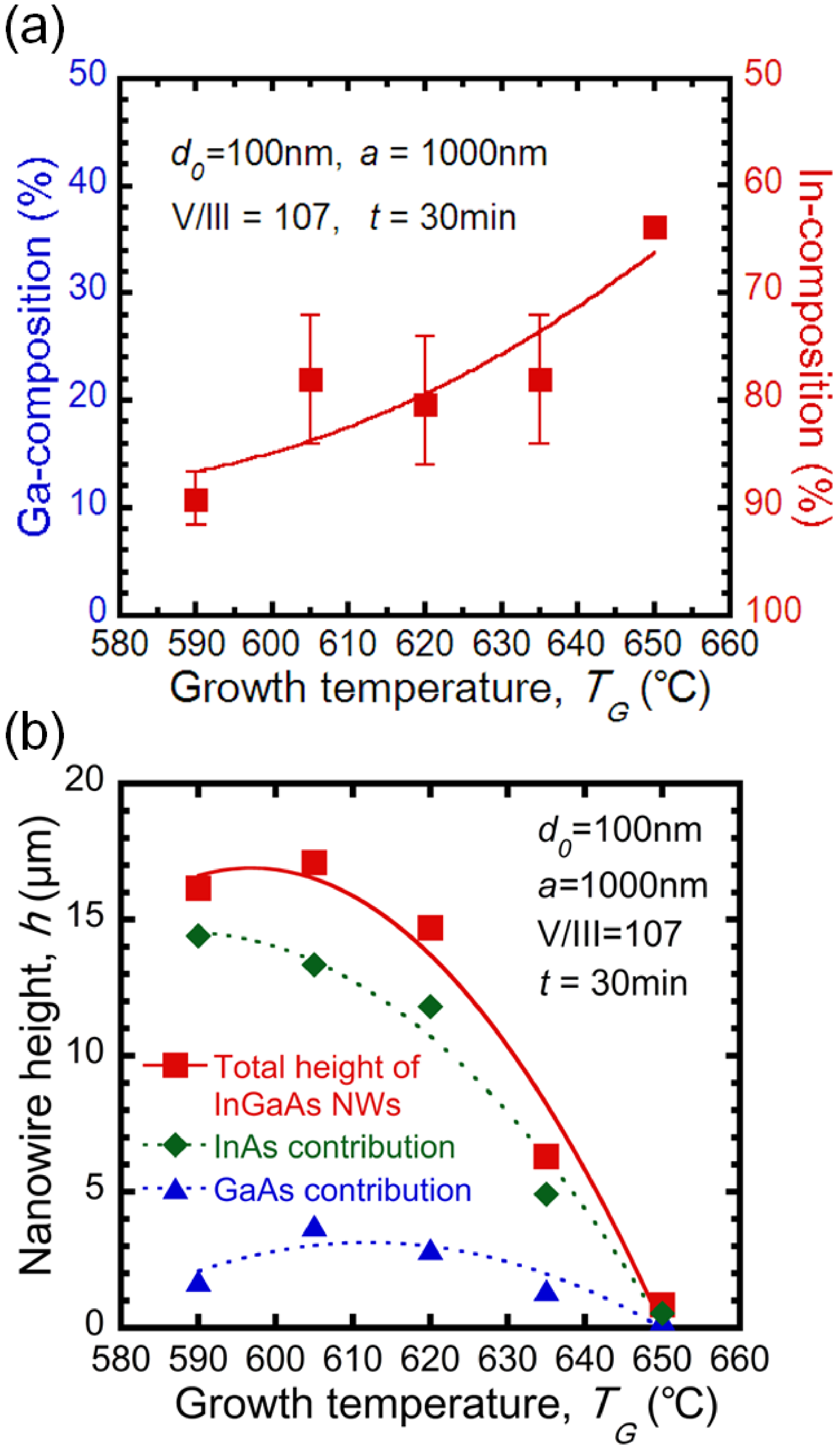
(a)
d_0=100nm, a = 1000nm
V/III = 107, t = 30min
Ga-composition (%)
0
10
20
30
40
50
In-composition (%)
50
60
70
80
90
100
580
590
600
610
620
630
640
650
660
Growth temperature, T_G (℃)
(b)
d_0=100nm
a=1000nm
V/III=107
t = 30min
Nanowire height, h (μm)
0
5
10
15
20
Total height of InGaAs NWs
InAs contribution
GaAs contribution
580
590
600
610
620
630
640
650
660
Growth temperature, T_G (℃)

Figure 5

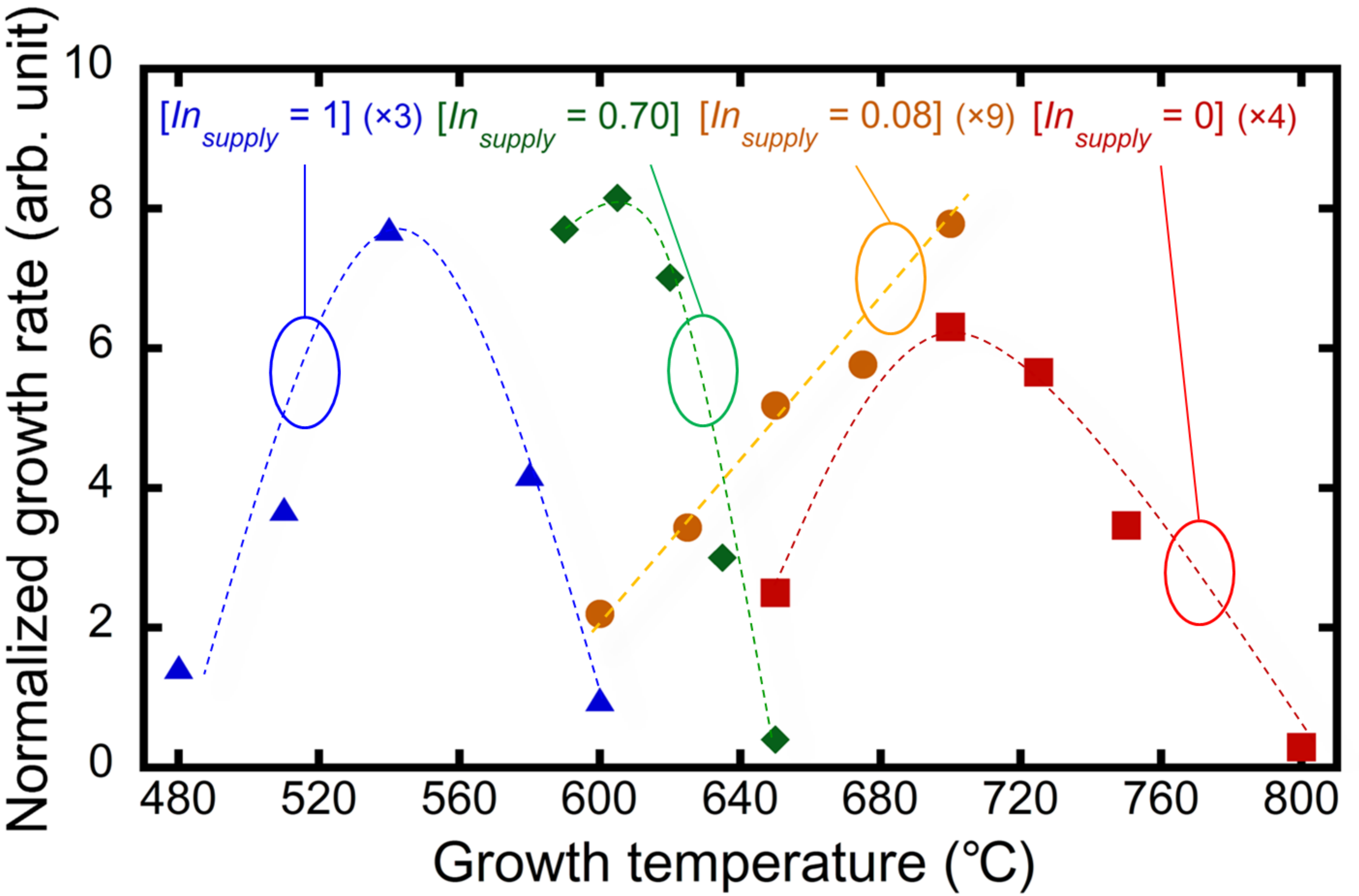

[In supply = 1] (×3)
[In supply = 0.70]
[In supply = 0.08] (×9)
[In supply = 0] (×4)
Normalized growth rate (arb. unit)
0
2
4
6
8
10
480
520
560
600
640
680
720
760
800
Growth temperature (°C)